Pion partonic distributions in a statistical model from pion-induced Drell-Yan and J/Ψ production data

Claude Bourrely,[1] Wen-Chen Chang,[2] and Jen-Chieh Peng[3]

[1]*Aix Marseille Univ, Université de Toulon, CNRS, CPT, Marseille, France*
[2]*Institute of Physics, Academia Sinica, Taipei 11529, Taiwan*
[3]*Department of Physics, University of Illinois at Urbana-Champaign, Urbana, Illinois 61801, USA*

(Received 23 February 2022; accepted 6 April 2022; published 26 April 2022)

We present a new analysis to extract pion parton distribution functions (PDFs) within the framework of the statistical model. Starting from the statistical model first developed for the spin-1/2 nucleon, we extend this model to describe the spin-0 pion. Based on a combined fit to both the pion-induced Drell-Yan data and the pion-induced J/Ψ production data, a new set of pion PDFs has been obtained. The inclusion of the J/Ψ production data in the combined fit has provided additional constraints for better determining the gluon distribution in the pion. We also compare the pion PDFs obtained in the statistical model with other existing pion PDFs.

DOI: 10.1103/PhysRevD.105.076018

I. INTRODUCTION

The description of proton parton distribution functions (PDFs) in terms of a statistical model approach, initiated 20 years ago [1], has provided pertinent insights on the flavor, spin, and momentum dependencies of the partonic constituents of the proton. An important feature of the statistical model is the natural connection between the valence and the sea quark distributions through the correlations in their Fermi-Dirac momentum distributions. The proton PDFs obtained in the statistical model can describe existing deep inelastic scattering (DIS) and Drell-Yan (DY) data very well. The statistical model approach also led to many successful predictions [2], including the flavor asymmetries of $\bar{d}(x) > \bar{u}(x)$ for the unpolarized sea [3–7] and $\Delta\bar{u}(x) > 0 > \Delta\bar{d}(x)$ for the polarized sea [8,9]. An updated overview of the major results obtained in the statistical model for describing the nucleon parton distributions can be found in [10].

The success of the statistical model for understanding many characteristics of the proton PDFs naturally suggests the feasibility of extending this approach to describe the partonic structures of other hadrons. Of particular importance are the partonic structures of pion and kaon, which have attracted much attention recently. As the lightest quark-antiquark bound state as well as a Goldstone boson due to the spontaneous breaking of the chiral symmetry, the pion is a unique hadronic system for exploring nonperturbative aspects of QCD.

The mounting interest in the partonic structure of pion is reflected in many recent studies under various theoretical frameworks including the chiral-quark model [11–13], Nambu-Jona-Lasinio model [14], light-front Hamiltonian [15,16], holographic QCD [17,18], maximum entropy method [19], and the continuum functional approach using Dyson-Schwinger equations (DSE) [20–25]. Moreover, a major advance in lattice QCD [26] has led several groups to perform calculations of the momentum (x) dependence of pion partonic distributions [27–34]. While the majority of these theoretical studies is focused on the pion valence quark distributions, recent DSE approach has also calculated the sea-quark and gluon distributions of pion [25].

On the experimental side, new information on the pion PDFs has been obtained in the COMPASS experiment with pion-induced dimuon production [35,36]. Additional measurements aiming at improved accuracy are planned for the future AMBER experiment at CERN [37]. Another experimental approach for probing pion PDFs is the tagged deep-inelastic scattering (TDIS) involving the DIS off the pion cloud via the Sullivan process [38]. The TDIS approach is being pursued at the Jefferson Laboratory [39] and planned for the future Electron-Ion Collider (EIC) [40]. The interest in pion partonic structure has also led to several recent extractions of pion PDFs via global fits to various existing data [41–45]. Until recently, knowledge of the pion PDFs was limited to global analyses performed more than two decades ago: OW [46], ABFKW [47], SMRS [48], GRV [49], and GRS [50]. These analyses were based mostly on pion-induced Drell-Yan and prompt-photon production data. New global analyses were performed recently, using

Drell-Yan data in BS [42] as well as both the Drell-Yan and direct-photon data in xFitter [51]. The analysis of JAM [41] included both the Drell-Yan data and the leading-neutron tagged electroproduction data.

The first extraction of the pion's PDFs based on the statistical model approach was reported in [42]. This work was followed by another recent analysis performed by BBP [44] which significantly reduced the number of parameters by imposing some constraints based on symmetry principles. This new analysis shows that a good description of the existing π^--induced Drell-Yan data can be obtained in the statistical model approach with a reduced number of parameters.

As the pion-induced Drell-Yan cross sections are dominated by $\bar{q}-q$ annihilation, they essentially probe the valence quark distribution in the pion, but leave the sea and the gluon distributions largely unconstrained. Two recent studies [52,53] showed that the existing pion-induced J/Ψ production data can impose useful additional constraints on the pion PDFs. Utilizing the theoretical frameworks of the color evaporation model (CEM) as well as the nonrelativistic QCD (NRQCD), it was found that existing pion-induced J/Ψ production data are sensitive to pion gluon distribution at relatively large x region. This result suggests the importance of including existing pion-induced J/Ψ production data in a global fit to extract the pion PDFs. In this paper, we present a new extraction of pion PDFs in the framework of statistical model via a global fit to both the Drell-Yan and the J/Ψ production data with pion beam.

II. PARAMETRIZATIONS OF MESON PDFS IN THE STATISTICAL MODEL

We begin by defining the notations of the various parton distribution functions for pions. After imposing the particle-antiparticle charge-conjugation (C) symmetry for the parton distributions in charged pions, we can define the PDFs of π^+ and π^- as follows:

$$U(x)\equiv u_{\pi^+}(x)=\bar{u}_{\pi^-}(x);\quad D(x)\equiv\bar{d}_{\pi^+}(x)=d_{\pi^-}(x). \tag{1}$$

$$\bar{U}(x)\equiv\bar{u}_{\pi^+}(x)=\bar{d}_{\pi^-}(x);\quad \bar{D}(x)\equiv d_{\pi^+}(x)=u_{\pi^-}(x). \tag{2}$$

$$S(x)\equiv s_{\pi^+}(x)=\bar{s}_{\pi^-}(x);\quad \bar{S}(x)\equiv\bar{s}_{\pi^+}(x)=s_{\pi^-}(x). \tag{3}$$

$$G(x)\equiv g_{\pi^+}(x)=g_{\pi^-}(x). \tag{4}$$

The requirements of charge-conjugation (C) and charge symmetry (CS) invariance would significantly reduce the number of independent parton distributions of pion. As shown in Eq. (1), C symmetry leads to $u_{\pi^+}(x)=\bar{u}_{\pi^-}(x)$. Invariance under the rotation in the isospin space by 180°, i.e., CS invariance [54], would give $\bar{u}_{\pi^-}(x)=\bar{d}_{\pi^+}(x)$. Therefore, invariance under the combined operations of C and CS implies $U(x)=D(x)$. In a similar fashion, it can be readily shown that $\bar{U}(x)=\bar{D}(x)$ and $S(x)=\bar{S}(x)$ [44].

Based on the framework of the statistical model, the four independent pion parton distributions are expressed in the following parametric forms:

$$xU(x)=xD(x)=\frac{A_U X_U x^{b_U}}{\exp[(x-X_U)/\bar{x}]+1}+\frac{\tilde{A}_U x^{\tilde{b}_U}}{\exp(x/\bar{x})+1}. \tag{5}$$

$$x\bar{U}(x)=x\bar{D}(x)=\frac{A_U (X_U)^{-1} x^{b_U}}{\exp[(x+X_U)/\bar{x}]+1}+\frac{\tilde{A}_U x^{\tilde{b}_U}}{\exp(x/\bar{x})+1}. \tag{6}$$

$$xS(x)=x\bar{S}(x)=\frac{\tilde{A}_U x^{\tilde{b}_U}}{2[\exp(x/\bar{x})+1]}. \tag{7}$$

$$xG(x)=\frac{A_G x^{b_G}}{\exp(x/\bar{x})-1},\qquad b_G=1+\tilde{b}_U. \tag{8}$$

Following the formulation developed for proton's PDFs, the x distributions for fermions (quark and antiquark) have Fermi-Dirac parametric form, while gluon has a Bose-Einstein x distribution [1,2]. The two terms for $xU(x)$ and $x\bar{U}(x)$ in Eqs. (5) and (6) refer to the nondiffractive and diffractive contribution, respectively [1,2]. As shown in the analysis of proton PDFs in the statistical model [2], the presence of the diffractive term is important for describing the data at the low x region.

A key feature of the statistical model is that the chemical potential, X_U, for the quark distribution $U(x)$ becomes $-X_U$ for the antiquark distribution $\bar{U}(x)$. The parameter $\bar{x}$ plays the role of the effective "temperature." For the strange-quark distribution $S(x)$, the requirement that $S(x)$ and $\bar{S}(x)$ have identical x distribution implies that the chemical potential in the nondiffractive term must vanish. Hence, the nondiffractive and diffractive terms for $S(x)$ have the same parametric form, and we make the simple assumption that $S(x)$ is equal to half of the diffractive part of $\bar{U}(x)$ due to the heavier strange quark mass. The expression $b_G=1+\tilde{b}_U$ in Eq. (8) has the interesting consequence that $G(x)$ has an identical x dependence as the diffractive part of the quark distributions when $x\to 0$. The dominance of the gluon and sea-quark distributions at $x\to 0$ and the strong interplay between them make this a very reasonable assumption.

Equations (5)–(8) contain a total of 7 parameters, namely, A_U, X_U, b_U, $\bar{x}$, $\tilde{A}_U$, $\tilde{b}_U$, and A_G. These parameters are also constrained by two sum rules, namely, the valence-quark number sum rule and the momentum sum rule:

$$\int_0^1 [U(x) - \bar{U}(x)]dx = 1,$$

$$\int_0^1 x[2U(x) + 2\bar{U}(x) + 2S(x) + G(x)]dx = 1. \quad (9)$$

III. GLOBAL FIT PROCEDURE

In order to obtain the parameters for pion PDFs according to the parametrizations listed in Eqs. (7)–(10), we have fitted both the Drell-Yan and the J/Ψ production data. For the Drell-Yan data, we have performed next-to-leading-order (NLO) QCD calculation to fit π^--induced dimuon production data on tungsten targets from E615 at 252 GeV [55], E326 at 225 GeV [56], and NA10 at 194 GeV and 286 GeV [57]. Detailed expressions for the NLO Drell-Yan cross sections were presented in [42]. The nucleon PDFs used in the calculation were taken from the BS15 PDFs [10], obtained from a global fit to existing data in the framework of the statistical model. The QCD evolution was performed using the HOPPET program [58], and the CERN MINUIT program [59] was utilized for the χ^2 minimization. Since the Drell-Yan data in this analysis were all collected using nuclear targets (tungsten), it is necessary to take into account the nuclear modification of the nucleon PDFs, described in [44].

For the analysis of the J/Ψ production data, we follow the recent study [53] on the comparison between pion-induced J/ψ production data with theoretical model calculations using the nonrelativistic QCD (NRQCD) [60] approach. The NRQCD approach is based on the factorization of the heavy-quark $Q\bar{Q}$ pair production and its subsequent hadronization. The production of the $Q\bar{Q}$ pair involves short-distance partonic interaction, calculated using perturbative QCD. The probability of a $Q\bar{Q}$ pair hadronizing into a quarkonium bound state is described by the long-distance matrix elements (LDMEs). The LDMEs, assumed to be universal, are determined from the experimental data [53,61].

We briefly describe the NRQCD framework used in this study as formulated in Ref. [61,62]. The differential cross section with respect to Feynman x (x_F), $d\sigma/dx_F$, for a charmonium state H ($H = J/\psi$, $\psi(2S)$, or χ_{cJ}) from the hN collisions, where h is the beam hadron and N the target nucleon, is [62]

$$\frac{d\sigma^H}{dx_F} = \sum_{i,j=q,\bar{q},G} \int_0^1 dx_1 dx_2 \delta(x_F - x_1 + x_2) \times f_i^h(x_1, \mu_F) f_j^N(x_2, \mu_F) \hat{\sigma}[ij \to H], \quad (10)$$

where i and j label the type of interacting partons (gluons, quarks and antiquarks), f^h and f^N are the incoming hadron and the target nucleon parton distribution functions, evaluated for their respective Bjorken-x values, x_1 and x_2 at the factorization scale μ_F. $\hat{\sigma}$ is given as

$$\hat{\sigma}[ij \to H] = \sum_n C^{ij}_{c\bar{c}[n]}(x_1 P_h, x_2 P_N, \mu_F, \mu_R, m_c) \times \langle \mathcal{O}_n^H[^{2S+1}L_J] \rangle, \quad (11)$$

where $C^{ij}_{c\bar{c}[n]}$ denotes the hard-process cross section for producing a $c\bar{c}$ pair with color (n), spin (S), orbital angular momentum (L) and total angular momentum (J). The hadronization probability is specified by the LDMEs, $\langle \mathcal{O}_n^H[^{2S+1}L_J] \rangle$. Here m_c and $M_{c\bar{c}}$ are the charm quark and $c\bar{c}$ pair masses, and μ_R is the renormalization scale.

The LDMEs used in the NRQCD calculation were taken from a recent study [53], which extracts these matrix elements by performed a fit to the energy dependence of the x_F-integrated J/Ψ production cross sections induced by proton and pion beams at fixed-target energies. Several sets of the LDMEs were obtained in this work, and we select the "Fit-2" solution for the LDMEs [53]. Using this set of LDMEs, the direct production cross sections of J/Ψ, $\Psi(2S)$ and the three χ_{cJ} states are calculated using Eq. (10). Furthermore, both the direct production of J/ψ and the feed-down from hadronic decays of $\psi(2S)$ and radiative decays of three χ_{cJ} states have been included for calculating the total J/ψ cross section. More details on the NRQCD calculation can be found in [53]. We found that the results of the present analysis are not sensitive to the choice of the specific LDME set obtained in [53], since they were all constrained by the same J/Ψ production data.

While there exist a significant number of measurements for pion-induced J/Ψ production cross sections as tabulated in [52], a large fraction of these data were collected using nuclear targets. Since large nuclear effects for J/Ψ production were found with both the proton and pion beams, we only select $\pi^- + p \to J/\Psi$ data in our global fit. This eliminates the uncertainties associated with the nuclear effects in J/Ψ production. The two $\pi^- + p \to J/\Psi$ experiments are the CERN WA39 experiment at 39.5 GeV [63], and the CERN NA3 experiment at 150, 200, and 280 GeV [64,65].

The CERN WA39 Collaboration measured the J/Ψ production cross section with 39.5 GeV hadron beams [63]. Data for the liquid H_2 target were taken with negative and positive hadron beams ($\pi^\pm$, $K^\pm$, p and $\bar{p}$). The differential cross sections in x_F for $\pi^- + p \to J/\Psi$ cover the region $0.05 \le x_F \le 0.85$. The normalization uncertainty on the cross sections is 15%.

The CERN NA3 experiment [64], has the largest pion-induced J/Ψ production statistics available to date. Data were collected at three different incident momenta, 150, 200, and 280 GeV. For all three beam energies, the cross sections have a normalization uncertainty of 13%. Although the numerical values of the cross sections were not listed in the NA3 publication, they can be retrieved

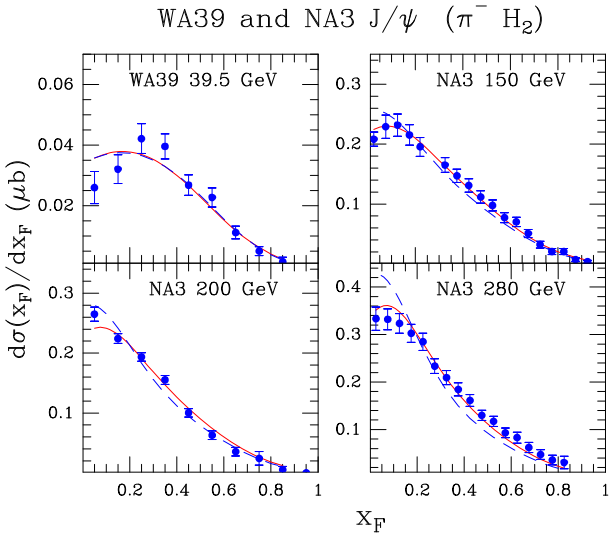

FIG. 1. J/ψ production data from the WA39 and NA3 experiment $\pi^- H_2$ at $P^{\pi}_{lab} = 39.5, 150, 200, 280$ GeV for $d\sigma/dx_F$ (blue circles) compared with the calculation of the BBP pion PDFs [44] (dashed blue curves). The solid red curves are results using the new pion PDFs.

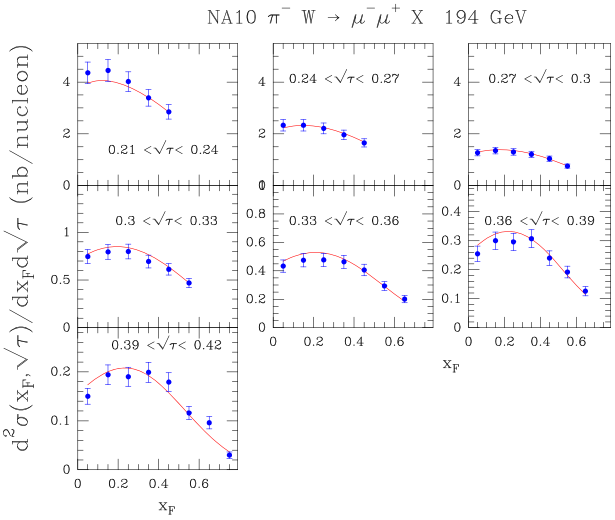

FIG. 2. Drell-Yan data from the NA10 experiment $\pi^- W$ at $P^{\pi}_{lab} = 194$ GeV [57]. $d^2\sigma/d\sqrt{\tau}dx_F$ versus x_F for several $\sqrt{\tau}$ intervals, where $\tau = m^2/s$, are compared with the results of the new fit (solid curves).

from the figures in the published paper [64] and an unpublished thesis [65].

IV. RESULTS OF THE GLOBAL FIT

Before presenting the results of the global fit, it is instructive to compare the J/Ψ production data with calculations using the recent pion PDFs obtained in the statistical model [44]. These pion PDFs were capable of reproducing the pion-induced Drell-Yan data very well. Since these Drell-Yan data are mostly sensitive to the valence-quark distributions, the gluon distribution in pion is only loosely constrained from the momentum sum rule [44]. Figure 1 shows the comparison between the data and the NRQCD calculation. While the agreement between data and calculation is acceptable for the WA39 data at 39.5 GeV ($\chi^2/ndp = 1.16$, where ndp is the number of data points), a much larger value of $\chi^2/ndp = 3.11$ is obtained for the NA3 data at higher pion beam energies. The J/Ψ production at 39.5 GeV is dominated by the $q\bar{q}$ annihilation process and is only sensitive to the valence-quark distribution in the pion [52,53]. As the valence-quark distribution is rather well determined from the BBP fit to the Drell-Yan data [44], it is reassuring that the J/Ψ data at 39.5 GeV is well described by the NRQCD calculation. In contrast, the gluon-gluon fusion process has increasing

TABLE I. Values of the K factor, χ^2 and χ^2/ndp (where ndp is the number of data points) for each dataset obtained from a global fit. P is the beam momentum, K the normalization factor to be multiplied by the calculation for the Drell-Yan and J/Ψ cross sections, N_{data} the number of data points, χ^2 and the χ^2/ndp.

Experiment	P(GeV)	K	N_{data}	χ^2	χ^2/ndp
E615	252	0.94	91	125	1.37
E326	225	1.07	50	77	1.53
NA10	286	1.12	23	10	0.44
NA10	194	1.14	44	22	0.49
WA39 J/ψ	39	0.63	9	11	1.22
NA3 J/ψ	150	1.13	18	9.6	0.53
NA3 J/ψ	200	0.92	9	14	1.56
NA3 J/ψ	280	1.00	17	17	1.0
Total			261	284	1.09

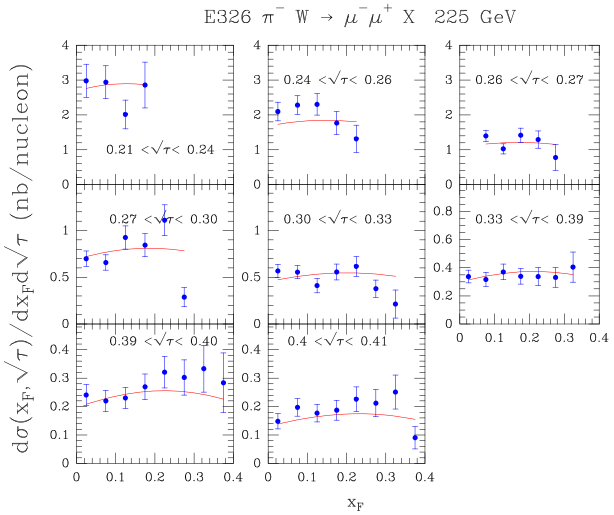

FIG. 3. Drell-Yan data from the E326 experiment $\pi^- W$ at $P^{\pi}_{lab} = 225$ GeV [56]. $d^2\sigma/d\sqrt{\tau}dx_F$ versus x_F for several $\sqrt{\tau}$ intervals are compared with the results of the new fit (solid curves).

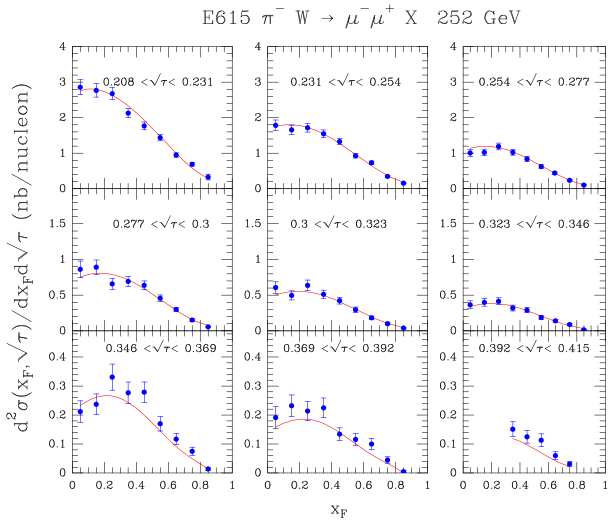

FIG. 4. Drell-Yan data from the E615 experiment $\pi^- W$ at $P^{\pi}_{lab} = 252$ GeV [55]. $d^2\sigma/d\sqrt{\tau}dx_F$ versus x_F for several $\sqrt{\tau}$ intervals are compared with the results of the new fit (solid curves).

important contributions as the pion beam energy increases [52,53]. The poor agreement between the calculation and the NA3 data at higher beam energies clearly indicates that the gluon distribution obtained from the fit to Drell-Yan data alone is not adequate. Combining the Drell-Yan and J/Ψ data in the global fit, as shown later, could lead to an improved extraction of both the gluon and the valence-quark distributions in the pion.

Following the procedure described in Secs. II and III, the best-fit values for the various parameters in the statistical model are obtained. Table I lists the number of data points and the values of χ^2 for the best fit to these datasets. Note that the normalizations for the absolute cross sections from various experiments contain systematic uncertainties on the order of ∼15 percents. In the global fit, the normalizations

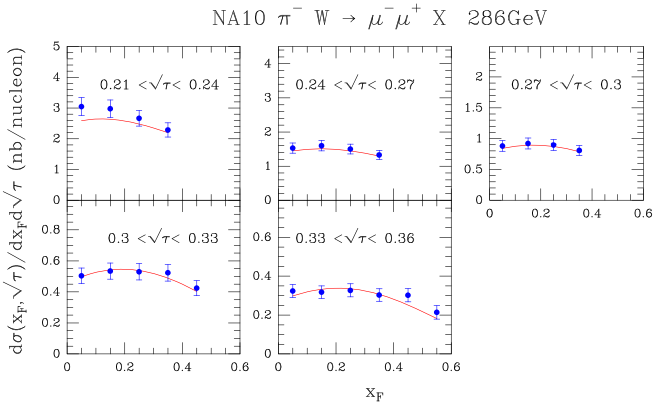

FIG. 5. Drell-Yan data from the NA10 experiment $\pi^- W$ at $P^{\pi}_{lab} = 286$ GeV [57]. $d^2\sigma/d\sqrt{\tau}dx_F$ versus x_F for several $\sqrt{\tau}$ intervals are compared with the results of the new fit (solid curves).

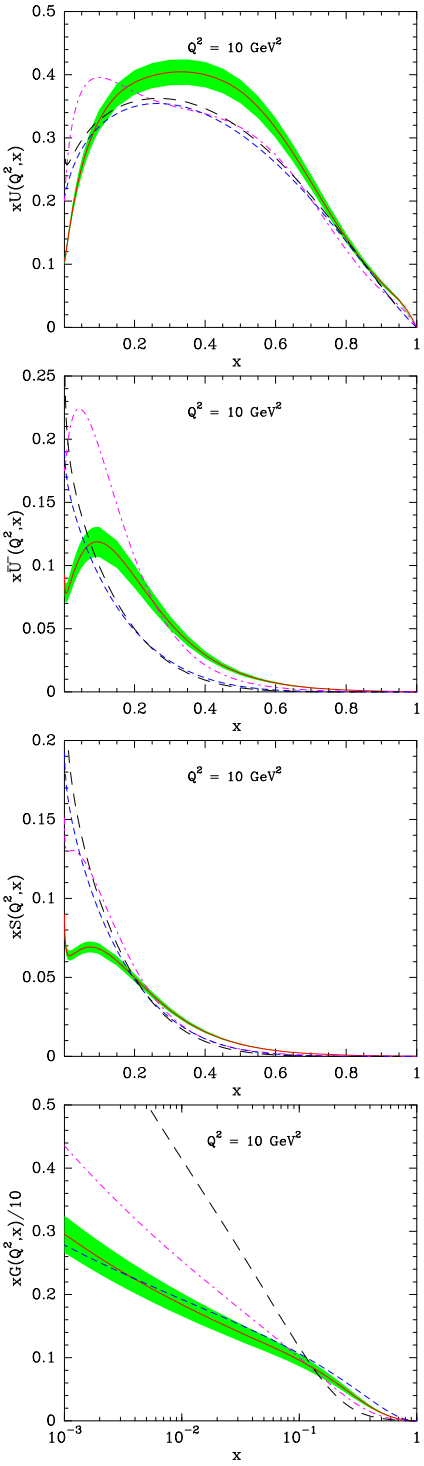

FIG. 6. Different π^- parton distributions, xU, $x\bar{U}$, xS, and xG, versus x, after NLO QCD evolution at $Q^2 = 10$ GeV^2. Present statistical model (solid, red), BBP PDF from Ref. [44] (dotted-dashed, violet), SMRS PDFs from Ref. [48] (dashed, blue), JAM PDFs from Ref. [45] (long-dashed, black) are shown. For SMRS $x\bar{S}(x) = x\bar{U}(x)$.

for various datasets are allowed to vary, as listed in Table I, in order to achieve improved consistency among various datasets. The result of the calculation is multiplied by the K

factor when compared with the data. We find that the K factors for the fit to Drell-Yan data are within 10% of unity, consistent with the normalization uncertainties of the experiments. For the J/Ψ data, the values of K factors are also found to be close to 1 for the NA3 data at three beam energies. However, the K factor for the WA39 experiment at 39 GeV is quite small, 0.63. A very similar finding was reported in the comparison between NRQCD calculation using previous pion PDFs with the J/Ψ production data [52]. This might reflect a slight underestimate of the normalization uncertainties from this experiment. It could also suggest that further improvement in the NRQCD model is warranted.

The χ^2 values listed in Table I shows that a simultaneous fit to the Drell-Yan and J/Ψ data in the statistical model with a small number of parameters can be obtained. In particular, the χ^2/ndp values are significantly smaller than that obtained with the previous pion PDFs [44]. Figure 1 shows the good agreement between the J/Ψ production data and the calculation with the new pion PDFs. In Figs. 2–5, the fits to the Drell-Yan data using the current result on pion's PDFs are displayed. We note that the Drell-Yan data remain well described by the statistical model, while much better agreement with the J/Ψ data is obtained with the new set of pion PDFs.

The best-fit parameters of the pion PDFs, obtained at an initial scale $Q_0^2 = 1$ GeV^2, are

$$\begin{aligned} A_U &= 1.11 \pm 0.05 \qquad & b_U &= 0.64 \pm 0.02 \\ X_U &= 0.72 \pm 0.01 \qquad & \bar{x} &= 0.119 \pm 0.002 \\ \tilde{A}_U &= 2.68 \pm 0.16 \qquad & \tilde{b}_U &= b_G - 1. \\ A_G &= 48.5 \pm 1.3 \qquad & b_G &= 1.88 \pm 0.04. \end{aligned} \tag{12}$$

It is worth noting that the temperature, $\bar{x} = 0.119$, found for pion is very close to that obtained for proton, $\bar{x} = 0.090$ [10], indicating a common feature for the statistical description for baryons and mesons. On the other hand, the chemical potential of the valence quark for pion, $X_U = 0.72$, is significantly large than that for proton, $X_U^+ = 0.475$, $X_U^- = 0.307$ [10].

TABLE II. Momentum fractions of valence quarks, sea quarks and gluons of various pion PDFs for π^- at the scale $Q^2 = 10$ GeV^2.

PDF	$\int_0^1 x\bar{u}_{\rm val}(x)dx$	$\int_0^1 x\bar{u}_{\rm sea}(x)dx$	$\int_0^1 xG(x)dx$
OW	0.176	0.026	0.488
ABFKW	0.178	0.026	0.468
SMRS	0.219	0.026	0.395
GRV	0.179	0.020	0.513
JAM[a]	0.222 ± 0.005	0.028 ± 0.002	0.367 ± 0.016
xFitter[a]	0.230 ± 0.008	0.036 ± 0.014	0.309 ± 0.065
BCP	0.242 ± 0.004	0.035 ± 0.002	0.326 ± 0.015

[a]Uncertainties estimated from the member PDF sets. BCP refers to the present work.

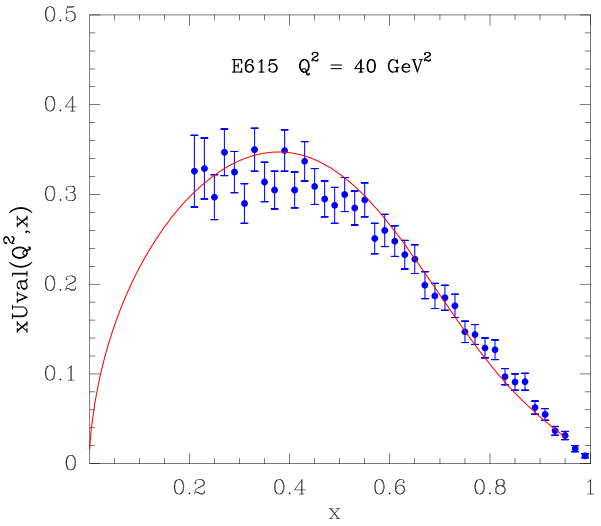

FIG. 7. The pion valence quark distribution $xU_{val}(x)$ deduced from the E615 Drell-Yan data [55] compared with the distribution obtained in the present analysis.

Figure 6 displays $xU(x)$, $x\bar{U}(x)$, $xS(x) = x\bar{S}(x)$, and $xG(x)$ at $Q^2 = 10$ GeV^2 obtained in the present analysis. Comparisons with the distributions from the previous analysis in the statistical model [44] and global fits of SMRS [48] and the more recent JAM [41] are also shown in Fig. 6. The shape and magnitude of the pion PDFs obtained in the statistical model analysis are different from that of SMRS and JAM. This reflects the very different parametric forms for the PDFs in the statistical model compared with that of the conventional global fits. We note that the gluon distribution of the new pion PDFs from this analysis is significantly larger than that of the JAM PDFs for the $x > 0.1$ region. Since the J/Ψ production data from NA3 is sensitive to the gluon distributions at the large x region, an improved determination of the gluon content in the pion is expected for the $x > 0.1$ region. Table II lists the momentum fractions carried by the quark, antiquark, and gluon in the pion for the new PDFs obtained in this work at $Q^2 = 10$ GeV^2. The corresponding momentum fractions for other pion PDFs are also shown for comparison. Figure 7 shows the extraction of the $xU_{val}(x)$ from the E615 Drell-Yan data [55] covering a very broad range of x. The E615 result is compared with the new pion PDF obtained in this analysis. Good agreement between the E615 data and the present pion PDFs is observed.

V. CONCLUSION AND FUTURE PROSPECTS

We have performed a new analysis to extract pion's PDFs in the statistical model via a global fit to existing π^--induced Drell-Yan data as well as the $\pi^- + p \to J/\Psi$ data. Using a parametrization of pion PDFs containing only a

few parameters, a good description of the Drell-Yan and J/Ψ production data can be obtained. The J/Ψ production data at the lowest pion beam energy, 39.5 GeV, are sensitive to the pion valence-quark distribution, analogous to the Drell-Yan data. At higher beam energies, the pion-induced J/Ψ production data probe the gluon distribution of pion. A combined analysis of the Drell-Yan and J/Ψ production data has provided an improved determination of both the valence-quark and the gluon distributions of pion compared with earlier studies.

From the new analysis, we confirm the previous result [44] that the statistical model approach gives very similar values for the temperature parameters for proton and pion, suggesting the consistency of this approach for different hadronic systems. A larger value of the valence-quark chemical potential for pion than for the proton is also found. New pion-induced Drell-Yan and J/Ψ production data anticipated from COMPASS and AMBER [37] would provide further tests of the pion PDFs obtained in the statistical approach.

The finding that both the Drell-Yan and J/Ψ production data can be well described with the statistical model approach suggests that this approach could be extended to extract the kaon PDFs [66]. While only a single low-statistics measurement of the kaon-induced Drell-Yan cross section is available [67], there exist additional kaon-induced J/Ψ production data at 39.5 GeV [63] and 200 GeV [64]. A combined analysis of these kaon-induced Drell-Yan and J/Ψ production might lead to a first extraction of the valence-quark and gluon distributions of kaon. The proposed RF separated kaon beam [37] at CERN would be extremely valuable for measuring the kaon PDFs in the future.

ACKNOWLEDGMENTS

We acknowledge interesting discussions with Prof. F. Buccella during the course of this work. This work was supported in part by the U.S. National Science Foundation Grant No. PHY-1812377 and the Ministry of Science and Technology in Taiwan, R.O.C.

[1] C. Bourrely, F. Buccella, and J. Soffer, A statistical approach for polarized parton distributions, Eur. Phys. J. C **23**, 487 (2002).
[2] C. Bourrely, F. Buccella, and J. Soffer, The statistical parton distributions: Status and prospects, Eur. Phys. J. C **41**, 327 (2005).
[3] A. Baldit *et al.*, Study of the isospin symmetry breaking in the light quark sea of the nucleon from the Drell-Yan process, Phys. Lett. B **332**, 244 (1994).
[4] E. A. Hawker *et al.*, Measurement of the Light Anti-Quark Flavor Asymmetry in the Nucleon Sea, Phys. Rev. Lett. **80**, 3715 (1998).
[5] J. C. Peng *et al.*, Anti-d/anti-u asymmetry and the origin of the nucleon sea, Phys. Rev. D **58**, 092004 (1998).
[6] R. S. Towell *et al.*, Improved measurement of the anti-d/anti-u asymmetry in the nucleon sea, Phys. Rev. D **64**, 052002 (2001).
[7] J. Dove *et al.*, The asymmetry of antimtter in the proton, Nature (London) **590**, 561 (2021).
[8] L. Adamczyk *et al.*, Measurement of the Longitudinal Spin Asymmetries for Weak Boson Production in Polarized Proton-Proton Collisions at RHIC, Phys. Rev. Lett. **113**, 072301 (2014).
[9] J. Adam *et al.*, Measurement of the longitudinal spin asymmetries for weak boson production in proton-proton collisions at $\sqrt{s} = 510$ GeV, Phys. Rev. D **99**, 051102 (2019).
[10] C. Bourrely an J. Soffer, New developments in the statistical approach of parton distributions: Tests and predictions up to LHC energies, Nucl. Phys. **A941**, 307 (2015).
[11] S. i. Nam, Parton-distribution functions for the pion and kaon in the gauge-invariant nonlocal chiral-quark model, Phys. Rev. D **86**, 074005 (2012).
[12] A. Watanabe, C. W. Kao, and K. Suzuki, Meson cloud effects on the pion quark distribution function in the chiral constituent quark model, Phys. Rev. D **94**, 114008 (2016).
[13] A. Watanabe, T. Sawada, and C. W. Kao, Kaon quark distribution functions in the chiral constituent quark model, Phys. Rev. D **97**, 074015 (2018).
[14] P. T. P. Hutauruk, I. C. Cloet, and A. W. Thomas, Flavor dependence of the pion and kaon form factors and parton distribution functions, Phys. Rev. C **94**, 035201 (2016).
[15] J. Lan, C. Mondal, S. Jia, X. Zhao, and J. P. Vary, Parton Distribution Functions from a Light Front Hamiltonian and QCD Evolution for Light Mesons, Phys. Rev. Lett. **122**, 172001 (2019).
[16] J. Lan, C. Mondal, S. Jia, X. Zhao, and J. P. Vary, Pion and kaon parton distribution functions from basis light front quantization and QCD evolution, Phys. Rev. D **101**, 034024 (2020).
[17] G. F. de Teramond, T. Liu, R. S. Sufian, H. G. Dosch, S. J. Brodsky, and A. Deur (HLFHS Collaboration), Universality of Generalized Parton Distributions in Light-Front Holographic QCD, Phys. Rev. Lett. **120**, 182001 (2018).
[18] A. Watanabe, T. Sawada, and M. Huang, Extraction of gluon distributions from structure functions at small x in holographic QCD, Phys. Lett. B **805**, 135470 (2020).
[19] C. Han, H. Xing, X. Wang, Q. Fu, R. Wang, and X. Chen, Pion valence quark distributions from maximum entropy method, Phys. Lett. B **800**, 135066 (2020).

[20] L. Chang, C. Mezrag, H. Moutarde, C. D. Roberts, J. Rodríguez-Quintero, and P. C. Tandy, Basic features of the pion valence-quark distribution function, Phys. Lett. B **737**, 23 (2014).
[21] L. Chang and A. W. Thomas, Pion valence-quark parton distribution function, Phys. Lett. B **749**, 547 (2015).
[22] C. Chen, L. Chang, C. D. Roberts, S. Wan, and H. S. Zong, Valence-quark distribution functions in the kaon and pion, Phys. Rev. D **93**, 074021 (2016).
[23] C. Shi, C. Mezrag, and H. s. Zong, Pion and kaon valence quark distribution functions from Dyson-Schwinger equations, Phys. Rev. D **98**, 054029 (2018).
[24] K. D. Bednar, I. C. Cloët, and P. C. Tandy, Distinguishing Quarks and Gluons in Pion and Kaon Parton Distribution Functions, Phys. Rev. Lett. **124**, 042002 (2020).
[25] M. Ding, K. Raya, D. Binosi, L. Chang, C. D. Roberts, and S. M. Schmidt, Symmetry, symmetry breaking, and pion parton distributions, Phys. Rev. D **101**, 054014 (2020).
[26] X. Ji, Parton Physics on a Euclidean Lattice, Phys. Rev. Lett. **110**, 262002 (2013); X. Ji, Y. S. Liu, Y. Liu, J. H. Zhang, and Y. Zhao, Large-momentum effective theory, Rev. Mod. Phys. **93**, 035005 (2021).
[27] J. H. Zhang, J. W. Chen, L. Jin, H. W. Lin, A. Schäfer, and Y. Zhao, First direct lattice-QCD calculation of the x-dependence of the pion parton distribution function, Phys. Rev. D **100**, 034505 (2019).
[28] R. S. Sufian, J. Karpie, C. Egerer, K. Orginos, J. W. Qiu, and D. G. Richards, Pion valence quark distribution from matrix element calculated in lattice QCD, Phys. Rev. D **99**, 074507 (2019).
[29] T. Izubuchi, L. Jin, C. Kallidonis, N. Karthik, S. Mukherjee, P. Petreczky, C. Shugert, and S. Syritsyn, Valence parton distribution function of pion from fine lattice, Phys. Rev. D **100**, 034516 (2019).
[30] B. Joó, J. Karpie, K. Orginos, A. V. Radyushkin, D. G. Richards, R. S. Sufian, and S. Zafeiropoulos, Pion valence structure from Ioffe-time parton pseudodistribution functions, Phys. Rev. D **100**, 114512 (2019).
[31] R. S. Sufian, C. Egerer, J. Karpie, R. G. Edwards, B. Joó, Y.-Q. Ma, K. Orginos, J.-W. Qiu, and D. G. Richards, Pion valence quark distribution from current-current correlation in lattice QCD, Phys. Rev. D **102**, 054508 (2020).
[32] X. Gao, L. Jin, C. Kallidonis, N. Karthik, S. Mukherjee, P. Petreczky, C. Shugert, S. Syritsyn, and Y. Zhao, Valence parton distribution of the pion from lattice QCD: Approaching the continuum limit, Phys. Rev. D **102**, 094513 (2020).
[33] C. Alexandrou, S. Bacchio, I. Cloët, M. Constantinou, K. Hadjiyiannakou, G. Koutsou, and C. Lauer (ETM Collaboration), Pion and kaon $\langle x3\rangle$ from lattice QCD and PDF reconstruction from Mellin moments, Phys. Rev. D **104**, 054504 (2021).
[34] Z. Fan and H. W. Lin, Gluon parton distribution of the pion from lattice QCD, Phys. Lett. B **823**, 136778 (2021).
[35] M. Aghasyan *et al.*, First Measurement of Transverse-Spin-Dependent Azimuthal Asymmetries in the Drell-Yan Process, Phys. Rev. Lett. **119**, 112002 (2017).
[36] C. Y. Hsieh, Expected statistical uncertainties of pion-induced Drell-Yan cross sections with tungsten target at COMPASS, J. Phys. Soc. Jpn. Conf. Proc. **26**, 031003 (2019).
[37] B. Adams *et al.*, Letter of intent: A new QCD facility at the M2 beam line of the CERN SPS (COMPASS++/AMBER), arXiv:1808.00848.
[38] J. D. Sullivan, One-pion exchange and deep-inelastic electron-nucleon scattering, Phys. Rev. D **5**, 1732 (1972).
[39] R. A. Montgomery *et al.*, Proposed measurement of tagged deep inelastic scattering in Hall A of Jefferson Lab, AIP Conf. Proc. **1819**, 030004 (2017).
[40] A. C. Aguilar *et al.*, Pion and kaon structure at the electron-ion collider, Eur. Phys. J. A **55**, 190 (2019).
[41] P. C. Barry, N. Sato, W. Melnitchouk, and C. R. Ji, First Monte Carlo Global QCD Analysis of Pion Parton Distributions, Phys. Rev. Lett. **121**, 152001 (2018).
[42] C. Bourrely and J. Soffer, Statistical approach of pion parton distributions from Drell-Yan process, Nucl. Phys. **A981**, 118 (2019).
[43] I. Novikov *et al.*, Parton distribution functions of the charged pion within the xFitter framework, Phys. Rev. D **102**, 014040 (2020).
[44] C. Bourrely, F. Buccella, and J. C. Peng, A new extraction of pion parton distributions in the statistical model, Phys. Lett. B **813**, 136021 (2021).
[45] P. C. Barry, C.-R. Ji, N. Sato, and W. Melnitchouk, Global QCD Analysis of Pion Parton Distributions with Threshold Resummation, Phys. Rev. Lett. **127**, 232001 (2021).
[46] J. F. Owens, Q^2-dependent parametrizations of pion parton distribution functions, Phys. Rev. D **30**, 943 (1984).
[47] P. Aurenche, R. Baier, M. Fontannaz, M. N. Kienzle-Focacci, and M. Werlen, The gluon content of the pion from high p_T direct photon production, Phys. Lett. B **233**, 517 (1989).
[48] P. J. Sutton, A. D. Martin, R. G. Roberts, and W. J. Stirling, Parton distributions for the pion extracted from Drell-Yan and prompt photon experiments, Phys. Rev. D **45**, 2349 (1992).
[49] M. Gluck, E. Reya, and A. Vogt, Pionic parton distributions, Z. Phys. C **53**, 651 (1992).
[50] M. Gluck, E. Reya, and I. Schienbein, Pionic parton distributions revisited, Eur. Phys. J. C **10**, 313 (1999).
[51] I. Novikov *et al.*, Parton distribution functions of the charged pion within the xFitter framework, Phys. Rev. D **102**, 014040 (2020).
[52] W. C. Chang, J. C. Peng, S. Platchkov, and T. Sawada, Constraining gluon density of pions at large x by pion-induced J/ψ production, Phys. Rev. D **102**, 054024 (2020).
[53] C. Y. Hsieh, Y. S. Lian, W. C. Chang, J. C. Peng, S. Platchkov, and T. Sawada, NRQCD analysis of charmonium production with pion and proton beams at fixed-target energies, Chin. J. Phys. **73**, 13 (2021).
[54] J. T. Londergan, J. C. Peng, and A. W. Thomas, Charge symmetry at the partonic level, Rev. Mod. Phys. **82**, 2009 (2010).
[55] J. S. Conway *et al.* (E615 Collaboration), Experimental study of muon pairs produced by 252-GeV pions on tungsten, Phys. Rev. D **39**, 92 (1989).
[56] H. B. Greenlee *et al.* (E326 Collaboration), Ph.D. Thesis, University of Chicago, 1985; Production of Massive Muon Pairs in π^--Nucleus Collisions Phys. Rev. Lett. **55**, 1555 (1985).

[57] B. Betev *et al.* (NA10 Collaboration), Experimental study of muon pairs produced by 252-GeV pions on tungsten, Z. Phys. C **28**, 9 (1985).
[58] C. P. Salam and J. Rojo, A higher order perturbative parton evolution toolkit (HOPPET), Comput. Phys. Commun. **180**, 120 (2009).
[59] F. James and M. Roos, CERN Program Library Long Writeup D506, 1994.
[60] G. T. Bodwin, E. Braaten, and G. P. Lepage, Rigorous QCD analysis of inclusive annihilation and production of heavy quarkonium, Phys. Rev. D **51**, 1125 (1995); **55**, 5853(E) (1997).
[61] M. Beneke and I. Z. Rothstein, Hadroproduction of quarkonia in fixed target experiments, Phys. Rev. D **54**, 2005 (1996); **54**, 7082(E) (1996).
[62] R. Vogt, The x(F) dependence of ψ and Drell-Yan production, Phys. Rev. C **61**, 035203 (2000).
[63] M. J. Corden *et al.*, Experimental Results on J/ψ production by $\pi^{\pm}$, $K^{\pm}$, p and $\bar{p}$ beams at 39.5-GeV, Phys. Lett. B **96**, 411 (1980).
[64] J. Badier *et al.*, Experimental J/Ψ hadronic production from 150-GeV/c to 280-GeV/c, Z. Phys. C **20**, 101 (1983).
[65] O. Callot, Production of high mass dimuons in experiment NA3, Ph.D. Thesis, Report No. LAL-81-05, 1981.
[66] J. C. Peng, W. C. Chang, S. Platchkov, and T. Sawada, Valence quark and gluon distributions of kaon from J/Psi production, arXiv:1711.00839.
[67] J. Badier *et al.*, Measurement of the K^-/π^- structure function ratio using the Drell-Yan process, Phys. Lett. B **93**, 354 (1980).